THE JOURNAL OF PHYSICAL CHEMISTRY Letters

pubs.acs.org/JPCL

# Observation of a Large-Scale Superstructure in Concentrated Hemoglobin Solutions by Using Small Angle Neutron Scattering

Andreas M. Stadler,*[,†,‡] Ralf Schweins,[†] Giuseppe Zaccai,[†] and Peter Lindner[†]

[†]Institut Laue Langevin, 38042 Grenoble, France, and [‡]Research Centre Jülich, 52425 Jülich, Germany

**ABSTRACT** We studied the properties of highly concentrated hemoglobin solutions from 137 to 290 mg/mL using small angle neutron scattering over a very large momentum transfer range from $q = 3.4 \times 10^{-4}$ to 0.16 Å$^{-1}$. The 137 and 227 mg/mL solutions revealed the presence of a large-scale superstructure with a radius of gyration on the order of 3000 Å. The 290 mg/mL solution was characterized by a mass fractal dimension of 2.67. Additionally, the scattering curve of the 290 mg/mL solution exhibited two shoulders, which might be due to the shape of the superstructure. In contrast, the radius of gyration of a single hemoglobin molecule is ~24 Å.

SECTION Macromolecules, Soft Matter

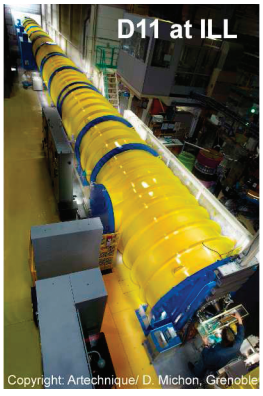


Proteins fulfill many important roles in biology, and much interest lies in a fundamental understanding of their properties and interactions under physiological conditions. Red blood cells (RBCs) are relatively simple cells. The main macromolecular component in RBCs is hemoglobin (Hb) at a concentration of ~330 mg/mL.[1] Hb solutions can be prepared at high purity and are excellent model systems to study the properties of proteins at high concentration close to physiological conditions. In previous protein solution studies, a sensitive balance between attractive and repulsive interactions was found to be important for the stability of concentrated solutions of binary crystallin mixtures.[2,3] The dependence of the attractive and repulsive interactions on the salt level was investigated for concentrated bovine serum albumin solutions.[4] A study reported that lysozyme forms small clusters at high concentration in the absence of salt,[5] but the interpretation of these data remains controversial.[6] We studied the properties of highly concentrated Hb solutions from 137 to 290 mg/mL using small angle neutron scattering (SANS) over a very large momentum transfer range from $3.4 \times 10^{-4}$ to 0.16 Å$^{-1}$. The experiments revealed the formation of a large-scale superstructure with increasing concentration. The solution at 290 mg/mL is characterized by a mass fractal dimension of 2.67, and the scattering curve exhibits two shoulders at $q' \sim 2.5 \times 10^{-3}$ and $q'' \sim 1.5 \times 10^{-2}$ Å$^{-1}$.

Measured data of the concentrated Hb solutions (137, 227, and 290 mg/mL) are shown in Figure 1. In general, the small angle scattering $I(q)$ of a protein solution is proportional to the product of the particle form factor $F(q)$ and the structure factor $S(q)$: $I(q) \sim F(q)^*S(q)$. The form factor $F(q)$ describes the shape of the particles averaged over all orientations. The structure factor $S(q)$ contains information about the interactions and correlations between the individual particles. In dilute solution, interparticle correlations are negligible, and $S(q) \sim 1$. In that case, the form factor of the macromolecule can be extracted readily.

Measured data of Hb at the high concentration of 137 mg/mL and at the dilute concentration of 4.8 mg/mL are compared in Figure 2. Data were normalized by the Hb concentration. Scattering of the dilute Hb solution can be described well with a simple spherical form factor.[7] We obtained a sphere radius of $R_S = 29.7 \pm 0.1$ Å corresponding to a radius of gyration of $R_G = (3/5)^{0.5} \cdot R_S = 23.0$ Å, which is reasonably close to the measured value of $23.7 \pm 0.5$ Å from the Guinier approximation.[8] The theoretical form factor was extended to smaller $q$ values, to illustrate the typical scattering behavior of a dilute Hb solution. In concentrated protein solutions, an analytical separation between $F(q)$ and $S(q)$ can sometimes be difficult, and will also depend on the model of the assumed interaction potential. In particular, this is the case when $F(q)$ contains not only a component of the Hb molecules but also a component of protein assemblies or clusters at small $q$ values.[6] The form factor of Hb is essentially constant below $10^{-2}$ Å$^{-1}$ in a log $I(q)$−log $q$ plot, as demonstrated in Figure 2. In concentrated protein solutions, the structure factor has got an interference peak at $q = 2\pi/d$, where $d$ is the average distance between individual Hb molecules.[1,9] The interference peak is clearly visible at $q \sim 0.1$ Å$^{-1}$ in Figure 1 at all measured Hb concentrations. In concentrated nonaggregating solutions of proteins, which do not form large-scale structures, the structure factor $S(q)$ tends toward a constant value below $10^{-2}$ Å$^{-1}$.[6,9] The upturn at $q < 0.05$ Å$^{-1}$ in all scattering curves in Figure 1 can thus

**Received Date:** May 6, 2010
**Accepted Date:** May 20, 2010
**Published on Web Date:** May 25, 2010





DOI: 10.1021/jz100576c | *J. Phys. Chem. Lett.* **2010**, *1*, 1805–1808

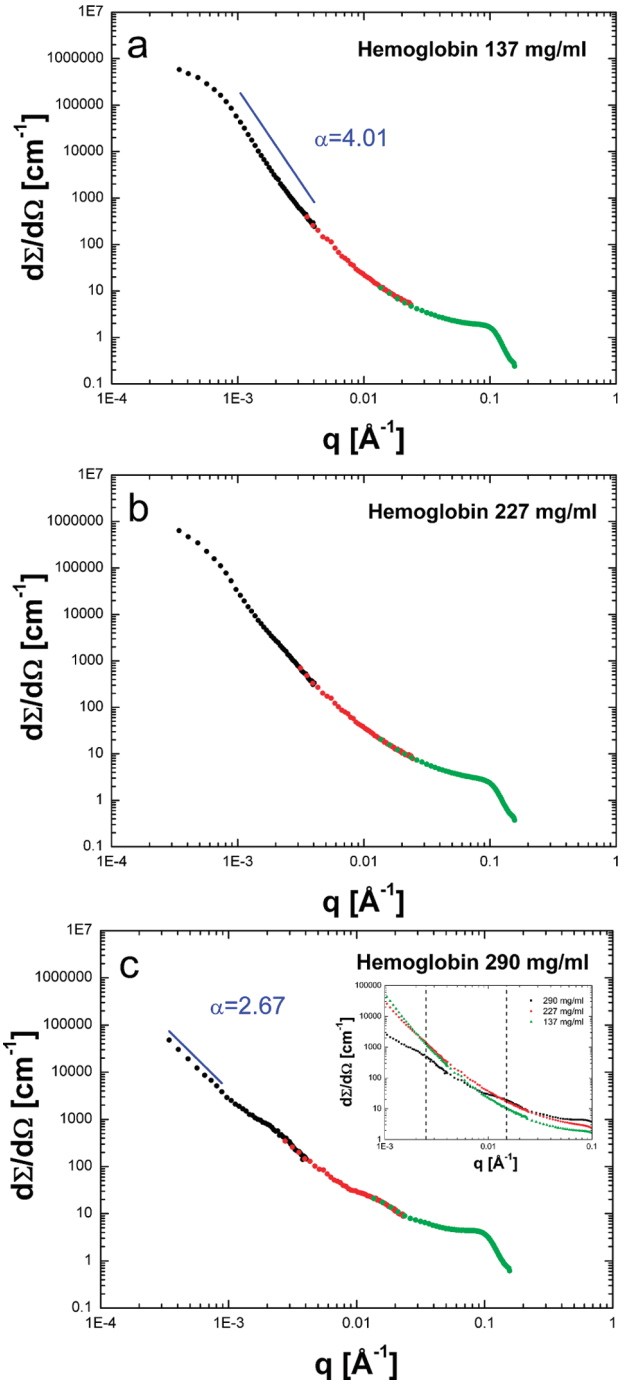


**Figure 1.** Measured SANS data of concentrated Hb solutions: (a) 137 mg/mL, (b) 227 mg/mL, and (c) 290 mg/mL. Blue straight lines represent characteristic power law behavior. Data points in black, red, and green (a,b,c) were measured with different instrument configurations on D11. The inset in panel c shows a magnification of the data and illustrates the emergence of both shoulders at $\sim 2.5 \times 10^{-3}$ and $\sim 1.5 \times 10^{-2}$ Å$^{-1}$ with increasing concentration.

only be explained by the formation of a large-scale superstructure of Hb molecules. In Figure 1a, at a concentration of 137 mg/mL, the measured intensity follows power-law behavior $I(q) \sim q^{-\alpha}$ between $\sim 1 \times 10^{-3}$ and $\sim 4 \times 10^{-3}$ Å

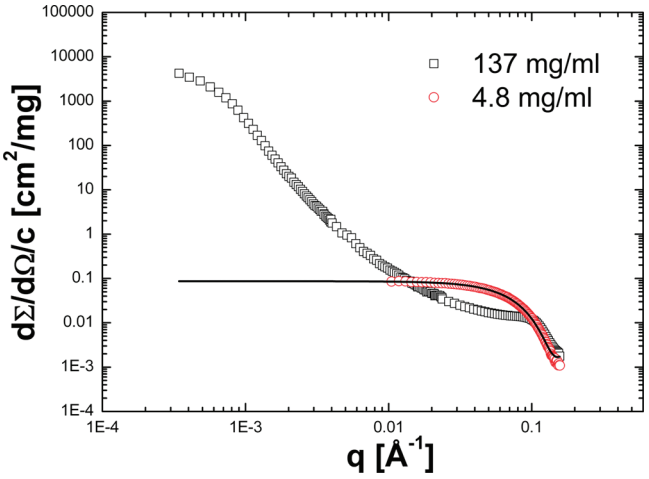


**Figure 2.** Experimental data of Hb at 137 mg/mL and 4.8 mg/mL. The black solid line is a fit to the measured intensities of 4.8 mg/mL with a spherical form factor. Data were normalized by the protein concentration. Black data points were measured on D11, red data points were measured on D22.

with $\alpha = 4.01 \pm 0.01$. At $q > 4 \times 10^{-3}$ Å$^{-1}$, the Hb−Hb interparticle correlations start to be seen, and the scattering curve deviates from power-law behavior. A radius of gyration $R'_G = 3060 \pm 460$ Å was estimated at 137 mg/mL between $3.4 \times 10^{-4}$ and $6.5 \times 10^{-4}$ Å$^{-1}$ with an interval of $1.1 < qR'_G < 2.0$. A power-law coefficient of $\alpha = 4$ indicates that the interface of the superstructure is sharp, and the object is compact. At 227 mg/mL (Figure 1b), the radius of gyration $R'_G = 3860 \pm 900$ Å was tentatively deduced between $3.4 \times 10^{-4}$ and $4.8 \times 10^{-4}$ Å$^{-1}$ with an interval of $1.3 < qR'_G < 1.9$.

We determine the number of Hb molecules that form the superstructure, and we neglect the fact that Hb molecules cannot completely fill the space due to closest packing restrictions. The number $N$ of individual Hb proteins in the large-scale superstructure can then be estimated by $N = (4\pi/3 \cdot R'^3_G)/(4\pi/3 \cdot R^3_G)$, where $R_G$ is the radius of gyration of Hb and $R'_G$ is the radius of gyration of the superstructure. We obtain $N \sim 2 \times 10^6$ at 137 mg/mL and $N \sim 4 \times 10^6$ at 227 mg/mL, where $N$ should only be considered as an upper limit and an order of magnitude estimate.

The apparent number $N'$ of Hb molecules that form the superstructures can also be estimated from the $I(0)/c$ values according to the method proposed by Jacrot and Zaccai.[10] This might be considered quite a severe approximation, as it neglects structure factor effects that are sure to be significant at the high concentrations. In any case, it is interesting to compare the values obtained with those of the volume calculation above. The ratio of $I(0)/c$ values for the different conditions is equal to the ratio of molar masses, provided the neutron wavelength is the same in the measurements. In our case, correction factors were applied as different neutron wavelengths were used in the measurements on D11 and D22.[11] The $I(0)/c$ values were obtained from the $I(q)/c$ by applying the Guinier approximation: $I(0)/c = 5880 \pm 200$ for $c = 137$ mg/mL, $I(0)/c = 5260 \pm 260$ for $c = 227$ mg/mL, and $I(0)/c = 0.0879 \pm 0.0001$ for $c = 4.8$ mg/mL. The molar mass ratios



DOI: 10.1021/jz100576c | J. Phys. Chem. Lett. 2010, 1, 1805–1808

between the concentrated and the diluted Hb solutions were $N' \sim 6.7 \times 10^4$ for the 137 mg/mL solution and $N' \sim 6.0 \times 10^4$ for the 227 mg/mL solution. In the case that all Hb molecules in the solutions form the superstructure, we would find $N \sim N'$. If a major fraction of all Hb molecules are in a liquid-like state and only a small part of all Hb proteins form the superstructure, then it would be $N \gg N'$. An estimation of the fraction $f$ of Hb molecules that actually form the superstructure might be obtained by $f = N'/N$. The numbers suggest that less than 10% of all Hb molecules form the superstructure in the concentrated solutions.

As the concentration of Hb increases, the scattering curve changes significantly. Two shoulders at $q' \sim 2.5 \times 10^{-3}$ Å$^{-1}$ and $q'' \sim 1.5 \times 10^{-2}$ Å$^{-1}$ are emerging and are most clearly visible at the highest concentration of 290 mg/mL (Figure 1c). The shoulder at $q' \sim 2.5 \times 10^{-3}$ Å$^{-1}$ may be due to the first subsidiary maximum of a sphere-like cluster with $R_G \sim 3000$ Å, as in the large-scale superstructure. The second shoulder at $q'' \sim 1.5 \times 10^{-2}$ Å$^{-1}$ might indicate the presence of a smaller superstructure with $R_G \sim 200$ Å. The shoulders might not be visible in the 137 and 227 mg/mL data, perhaps because of the relatively low concentration of the clusters.

Interestingly, the scattering curve of the 290 mg/mL Hb sample follows power-law behavior at the smallest $q$ values with $\alpha = 2.67 \pm 0.01$ (see Figure 1c). Fractal morphologies are sometimes found in disordered systems, such as polymer blends, colloidal gels, or silica aerogels.[12,13] In these systems, power-law scattering behavior at small $q$ values is observed, which is closely related to the self-similarity of the fractal structure. Small angle scattering experiments are excellently suited to study the properties of fractal systems, as the fractal dimension can be deduced directly from the measured power-law coefficient. Power-law coefficients with $\alpha < 3$ are characteristic signs for mass fractal morphologies.[14] At larger $q$ values, corresponding to smaller real space distances, the substructure of the system becomes visible, and the measured intensities deviate from power-law scattering. Measured data can be compared to simulations of different nonequilibrium growth processes. Simulations of diffusion limited aggregation in three dimensions yielded a power-law coefficient of $\alpha = 2.5$,[15] which is slightly smaller than the value found for the 290 mg/mL Hb solution. The larger fractal dimension of our experiment might indicate a denser and more compact structure as compared to idealized diffusion-limited aggregation.

Stradner and co-workers reported that, on average, around seven lysozyme molecules assemble into a small cluster at 15 °C and at a volume fraction of 0.2.[5] The Hb concentrations of 137, 227, and 290 mg/mL correspond to volume fractions of 0.10, 0.17, and 0.22, respectively. In this study we did not find signs of small equilibrium cluster formation as reported by Stradner et al.[5] It should be noted that the SANS study on lysozyme was performed in the absence of salt, whereas in our investigation the Hb solutions contained a moderate amount of salt, which screens electrostatic interactions. Lysozyme in solution is well known to form large crystals rapidly, even within 1 day,[16] whereas Hb solutions under similar conditions crystallize typically within some months.[17] The specific properties of lysozyme and Hb might contribute to the observed discrepancy.

The phase behavior of concentrated human Hb solutions between 330 and 500 mg/mL, and Hb in whole RBCs were investigated using rheology, colloid osmotic pressure, and micropipet experiments.[18,19] In these studies, the onset of Hb aggregation at body temperature was discovered. Circular dichroism[20] and incoherent neutron scattering experiments[21,22] revealed that Hb exhibits a loss of secondary structure at body temperature, which leads to a more flexible state of the protein. It was speculated that the partial loss of Hb structure reflects an increase in surface hydrophobicity, which might cause stronger protein−protein interactions and thus lead to protein aggregation.[21,23,24]

We expect that the observed Hb superstructure also exists in whole RBCs, as the Hb concentration of 290 mg/mL, the salt level and pD are rather similar to physiological conditions in cells. The presence of a large-scale Hb superstructure with mass fractal properties might provide the basis for body temperature-related Hb aggregation, and participate in biologically relevant oxygen transport properties of RBCs.

## MATERIALS AND METHODS

Human venous blood was taken with heparinized tubes. $H_2O$ and $D_2O$ HEPES buffer solutions at pH/pD 7.4 and 290 mOsm were saturated with CO to increase the stability of Hb (137 mM NaCl, 4 mM KCl, 1.8 mM $CaCl_2$, 0.8 mM $Na_2HPO_4$, 0.2 mM $NaH_2PO4$, 0.7 mM $MgSO_4$, 8.4 mM HEPES, and 4 mM NaOH). The pD was calculated by adding 0.4 to the value measured on a normally calibrated pH meter. The salt concentration was chosen to resemble conditions in whole cells.[25] The cells were washed twice with $H_2O$ HEPES buffer and collected at 560 relative centrifugal force (rcf) to remove plasma proteins. The RBC were repeatedly washed with $D_2O$ HEPES buffer until the level of $H_2O$ was estimated to be below 0.1%. The RBC were then lysed by adding 10% distilled $D_2O$ and centrifuged at 20 000 rcf for 20 min to remove cell membranes and nonlysed cells. The supernatant was centrifuged at 380 000 rcf for 1 h to remove any cell membrane fragments. Aliquots of the Hb solution were diluted with $D_2O$ HEPES buffer. The Hb solution samples were centrifuged at 20 000 rcf for 1 h shortly before the neutron scattering experiments. The final concentration of the Hb solutions was determined with UV/visible absorption. Hb concentrations were 290, 227, and 137 mg/mL. The purity of the Hb solutions was estimated to be higher than 99%. The salt in the solutions screens electrostatic interactions, and the pD was similar to physiological conditions[25] and close to the isoelectric point of Hb of pH 6.8.[26]

SANS of the Hb solutions was measured on the instruments D11 and D22, which are located at the Institut Laue-Langevin in Grenoble, France.[27] The relation between momentum transfer $q$, scattering angle $2\theta$, and neutron wavelength $\lambda$ is $q = 4\pi/\lambda \cdot \sin(\theta)$. On D11, the neutron wavelength was set to 20 Å, and three different instrument configurations were combined to cover a very large momentum transfer range from $q = 3.4 \times 10^{-4}$ to 0.16 Å$^{-1}$ (sample-to-detector distance of 39 m, collimation distance of 40.5 m; sample-to-detector distance of 8 m, collimation distance of 8 m; sample-to-detector distance of 1.2 m, collimation distance of 1.5 m).



DOI: 10.1021/jz100576c | J. Phys. Chem. Lett. 2010, 1, 1805–1808

On D22, a neutron wavelength of 6 Å, a sample-to-detector distance of 4 m and a collimation distance of 4 m were used. The covered momentum transfer range was $0.01 < q < 0.13$ $Å^{-1}$. The Hb solutions were measured in quartz cuvettes with 1 mm thickness at 14 °C on D11 and at 20 °C on D22. Temperature was controlled with a water bath. The scattering contribution of the empty quartz cuvettes was subtracted from the Hb samples. Data was scaled to absolute units, and the neutron detector was calibrated using a $H_2O$ measurement.[11]

## AUTHOR INFORMATION

### Corresponding Author:

*To whom correspondence should be addressed. E-mail: a.stadler@fz-juelich.de.

**ACKNOWLEDGMENT** We thank Stephan Förster for fruitful discussion and comments on data interpretation. A.M.S. thanks Gerhard Artmann, Georg Büldt, Ilya Digel, Peter Kayser, Dariusz Porst, and Aysegül Temiz-Artmann for continuous help and support.

## REFERENCES

(1) Krueger, S.; Nossal, R. SANS Studies of Interacting Hemoglobin in Intact Erythrocytes. *Biophys. J.* **1988,** *53*, 97–105.
(2) Dorsaz, N.; Thurston, G. M.; Stradner, A.; Schurtenberger, P.; Foffi, G. Colloidal Characterization and Thermodynamic Stability of Binary Eye Lens Protein Mixtures. *J. Phys. Chem. B* **2009,** *113*, 1693–1709.
(3) Stradner, A.; Foffi, G.; Dorsaz, N.; Thurston, G.; Schurtenberger, P. New Insight into Cataract Formation: Enhanced Stability through Mutual Attraction. *Phys. Rev. Lett.* **2007,** *99*, 1–4.
(4) Zhang, F.; Skoda, M. W.; Jacobs, R. M.; Martin, R. A.; Martin, C. M.; Schreiber, F. Protein Interactions Studied by SAXS: Effect of Ionic Strength and Protein Concentration for BSA in Aqueous Solutions. *J. Phys. Chem. B* **2007,** *111*, 251–259.
(5) Stradner, A.; Sedgwick, H.; Cardinaux, F.; Poon, W. C.; Egelhaaf, S. U.; Schurtenberger, P. Equilibrium Cluster Formation in Concentrated Protein Solutions and Colloids. *Nature* **2004,** *432*, 492–495.
(6) Shukla, A.; Mylonas, E.; Di Cola, E.; Finet, S.; Timmins, P.; Narayanan, T.; Svergun, D. Absence of Equilibrium Cluster Phase in Concentrated Lysozyme Solutions. *Proc. Natl. Acad. Sci. U.S.A.* **2008,** *105*, 5075–5080.
(7) Guinier, A.; Fournet, G. *Small-Angle Scattering of X-Rays*; John Wiley and Sons: New York, 1955.
(8) Schelten, J.; Schlecht, P.; Schmatz, W.; Mayer, A. Neutron Small Angle Scattering of Hemoglobin. *J. Biol. Chem.* **1972,** *247*, 5436–5441.
(9) Krueger, S.; Chen, S. H.; Hofrichter, J.; Nossal, R. Small Angle Neutron Scattering Studies of HbA in Concentrated Solutions. *Biophys. J.* **1990,** *58*, 745–757.
(10) Jacrot, B.; Zaccai, G. Determination of Molecular-Weight by Neutron-Scattering. *Biopolymers* **1981,** *20*, 2413–2426.
(11) Lindner, P. Water Calibration at D11 Verified with Polymer Samples. *J. Appl. Crystallogr.* **2000,** *33*, 807–811.
(12) Bhatia, S. R. Ultra-Small-Angle Scattering Studies of Complex Fluids. *Curr. Opin. Colloid Interface Sci.* **2005,** *9*, 404–411.
(13) Schaefer, D. W.; Keefer, K. D. Structure of Random Porous Materials: Silica Aerogel. *Phys. Rev. Lett.* **1986,** *56*, 2199–2202.
(14) Beaucage, G. Small-Angle Scattering from Polymeric Mass Fractals of Arbitrary Mass-Fractal Dimension. *J. Appl. Crystallogr.* **1996,** *29*, 134–146.
(15) Witten, T. A.; Sander, L. M. Diffusion-Limited Aggregation. *Phys. Rev. B* **1983,** *27*, 5686–5697.
(16) Pusey, M. L.; Snyder, R. S.; Naumann, R. Protein Crystal-Growth - Growth-Kinetics for Tetragonal Lysozyme Crystals. *J. Biol. Chem.* **1986,** *261*, 6524–6529.
(17) Perutz, M. F. Preparation of Haemoglobin Crystals. *J. Cryst. Growth* **1968,** *2*, 54–56.
(18) Artmann, G. M.; Digel, I.; Zerlin, K. F.; Maggakis-Kelemen, C.; Linder, P.; Porst, D.; Kayser, P.; Stadler, A. M.; Dikta, G.; Temiz Artmann, A. Hemoglobin Senses Body Temperature. *Eur. Biophys. J.* **2009,** *38*, 589–600.
(19) Artmann, G. M.; Kelemen, C.; Porst, D.; Büldt, G.; Chien, S. Temperature Transitions of Protein Properties in Human Red Blood Cells. *Biophys. J.* **1998,** *75*, 3179–3183.
(20) Artmann, G. M.; Burns, L.; Canaves, J. M.; Temiz-Artmann, A.; Schmid-Schonbein, G. W.; Chien, S.; Maggakis-Kelemen, C. Circular Dichroism Spectra of Human Hemoglobin Reveal a Reversible Structural Transition at Body Temperature. *Eur. Biophys. J.* **2004,** *33*, 490–496.
(21) Stadler, A. M.; Digel, I.; Artmann, G. M.; Embs, J. P.; Zaccai, G.; Büldt, G. Hemoglobin Dynamics in Red Blood Cells: Correlation to Body Temperature. *Biophys. J.* **2008,** *95*, 5449–5461.
(22) Stadler, A. M.; Digel, I.; Embs, J. P.; Unruh, T.; Tehei, M.; Zaccai, G.; Büldt, G.; Artmann, G. M. From Powder to Solution: Hydration Dependence of Human Hemoglobin Dynamics Correlated to Body Temperature. *Biophys. J.* **2009,** *96*, 5073–5081.
(23) Digel, I.; Maggakis-Kelemen, C.; Zerlin, K. F.; Linder, P.; Kasischke, N.; Kayser, P.; Porst, D.; Temiz Artmann, A.; Artmann, G. M. Body Temperature-Related Structural Transitions of Monotremal and Human Hemoglobin. *Biophys. J.* **2006,** *91*, 3014–3021.
(24) Zerlin, K. F.; Kasischke, N.; Digel, I.; Maggakis-Kelemen, C.; Temiz Artmann, A.; Porst, D.; Kayser, P.; Linder, P.; Artmann, G. M. Structural Transition Temperature of Hemoglobins Correlates with Species' Body Temperature. *Eur. Biophys. J.* **2007,** *37*, 1–10.
(25) Alberts, B.; Johnson, A.; Lewis, J.; Raff, M.; Roberts, K.; Walter, P. *Molecular Biology of the Cell*; Garland Science: New York, 2002.
(26) Conway-Jacobs, A.; Lewin, L. M. Isoelectric Focusing in Acrylamide Gels: Use of Amphoteric Dyes As Internal Markers for Determination of Isoelectric Points. *Anal. Biochem.* **1971,** *43*, 394–400.
(27) *The ILL Yellow Book*. http://www.ill.eu/instruments-support/instruments-groups/yellowbook/ (accessed May 2010).





DOI: 10.1021/jz100576c | *J. Phys. Chem. Lett.* **2010,** *1*, 1805–1808